

# Copper isotopes as monitors of redox processes in hydrothermal mineralization

Gregor Markl <sup>a,\*</sup>, Yann Lahaye <sup>b</sup>, Gregor Schwinn <sup>a</sup>

<sup>a</sup> *Institut für Geowissenschaften, Wilhelmstr. 56, D-72074 Tübingen, Germany*

<sup>b</sup> *Institut für Mineralogie, Senckenberganlage, D-60054 Frankfurt, Germany*

Received 14 October 2005; accepted in revised form 19 June 2006

## Abstract

The stable copper isotope composition of 79 samples of primary and secondary copper minerals from hydrothermal veins in the Schwarzwald mining district, South Germany, shows a wide variation in  $\delta^{65}\text{Cu}$  ranging from  $-2.92$  to  $2.41\text{‰}$ . We investigated primary chalcopyrite, various kinds of fahlores and emplectite, as well as supergene native copper, malachite, azurite, cuprite, tenorite, olivenite, pseudomalachite and chrysocolla. Fresh primary Cu(I) ores have at most localities copper isotope ratios ( $\delta^{65}\text{Cu}$  values) of  $0 \pm 0.5\text{‰}$  despite the fact that the samples come from mineralogically different types of deposits covering an area of about 100 by 50 km and that they formed during three different mineralization events spanning the last 300 Ma. Relics of the primary ores in oxidized samples (i.e., chalcopyrite relics in an iron oxide matrix with an outer malachite coating) display low isotope ratios down to  $-2.92\text{‰}$ . Secondary Cu(I) minerals such as cuprite have high  $\delta^{65}\text{Cu}$  values between 0.4 and 1.65‰, whereas secondary Cu(II) minerals such as malachite show a range of values between  $-1.55$  and  $2.41\text{‰}$ , but typically have values above  $+0.5\text{‰}$ . Within single samples, supergene oxidation of fresh chalcopyrite with a  $\delta$  value of 0‰ causes significant fractionation on the scale of a centimetre between malachite (up to 1.49‰) and relict chalcopyrite (down to  $-2.92\text{‰}$ ). The results show that—with only two notable exceptions—high-temperature hydrothermal processes did not lead to significant and correlatable variations in copper isotope ratios within a large mining district mineralized over a long period of time. Conversely, low-temperature redox processes seriously affect the copper isotope compositions of hydrothermal copper ores. While details of the redox processes are not yet understood, we interpret the range in compositions found in both primary Cu(I) and secondary Cu(II) minerals as a result of two competing controls on the isotope fractionation process: within-fluid control, i.e., the fractionation during the redox process among dissolved species, and fluid–solid control, i.e., fractionation during precipitation involving reactions between dissolved Cu species and minerals. Additionally, Rayleigh fractionation in a closed system may be responsible for some of the spread in isotope compositions. Our study indicates that copper isotope variations may be used to decipher details of natural redox processes and therefore may have some bearing on exploration, evaluation and exploitation of copper deposits. On the other hand, copper isotope analyses of single archeological artefacts or geological or biological objects cannot be easily used as reliable fingerprint for the source of copper, because the variation caused by redox processes within a single deposit is usually much larger than the inter-deposit variation.

© 2006 Elsevier Inc. All rights reserved.

## 1. Introduction

The reported natural variation of the ratio of the stable copper isotopes  $^{63}\text{Cu}$  and  $^{65}\text{Cu}$  is up to 9‰ (Walker et al., 1958; Shields et al., 1965; Marechal et al., 1999; Marechal

and Sheppard, 2002; Johnson et al., 2004; Zhu et al., 2000; Rouxel et al., 2004), where  $\delta$  is defined as

$$\delta^{65}\text{Cu} = \left[ \left( \frac{^{65}\text{Cu}}{^{63}\text{Cu}} \right)_{\text{sample}} / \left( \frac{^{65}\text{Cu}}{^{63}\text{Cu}} \right)_{\text{standard}} - 1 \right] \times 1000.$$

In the present study, the  $\delta^{65}\text{Cu}$  values are reported relative to the standard NIST SRM-976.

In chondrites, the maximum variation does not exceed 1.5‰, but three reservoirs presumably formed at high temperatures with significantly different compositions could be

\* Corresponding author. Fax: +49 7071 29 3060.

E-mail addresses: [markl@uni-tuebingen.de](mailto:markl@uni-tuebingen.de) (G. Markl), [lahaye@em.uni-frankfurt.de](mailto:lahaye@em.uni-frankfurt.de) (Y. Lahaye).

identified (Luck et al., 2003). These data together with oxygen isotopes and element ratios support the presence of isotopically distinct Cu components in the Solar System, which indicates that relatively high-temperature processes may be capable of altering Cu isotope compositions significantly. Similarly, Zhu et al. (2000) found for hydrothermal vents on the ocean floor a range of  $\delta^{65}\text{Cu}$  values between  $-0.5$  and  $+1.2\%$ . However, magmatic processes do not appear to produce significant copper isotope fractionation, although Zhu et al. (2002) showed that significant iron isotope fractionation occurs up to  $1000\text{ }^\circ\text{C}$ . Rouxel et al. (2004), however, explained the large  $\delta^{65}\text{Cu}$  variation in seafloor sulfide deposits by low-temperature secondary processes after sulfide deposition, while the primary, high-temperature (about  $350\text{ }^\circ\text{C}$ ) precipitation did not lead to significant variation in  $\delta^{65}\text{Cu}$ . In hydrothermal copper deposits formed between  $150$  and  $290\text{ }^\circ\text{C}$ , Jiang et al. (2002) report a variation in  $\delta^{65}\text{Cu}$  for chalcopyrite between  $-3.7$  and  $+0.3\%$ .

The natural variation of copper isotope ratios has been attributed to a number of processes such as liquid–vapor separation, multi-step equilibrium processes, redox reactions or involvement of organisms (Marechal et al., 1999; Zhu et al., 2000, 2002; Jiang et al., 2002; Larson et al., 2003; Graham et al., 2004; Rouxel et al., 2004; Ehrlich et al., 2005). Zhu et al. (2000) have shown that even samples of the same mineral from the same locality may exhibit large variations of copper isotope ratios. All workers agree that both biological and inorganic processes can cause significant shifts in copper isotope ratios at low temperatures (Gale et al., 1999; Marechal et al., 1999; Zhu et al., 2000, 2002; O’Nions and Zhu, 2002; Riuz et al., 2002; Marechal and Albarede, 2002; Larson et al., 2003; Graham et al., 2004). The details of the processes causing the  $\delta^{65}\text{Cu}$  variations are not yet clear in every case, but Graham et al. (2004) inferred for the Grasberg deposit, Australia, that selective metamorphic overprinting on the microscale was responsible for the variations in Cu and Fe isotope values observed. Their data indicate that variations of  $\delta^{65}\text{Cu}$  values in magmatic–hydrothermal porphyry copper systems and associated skarns range between  $0$  and  $1.3\%$  and that there is a distinctive evolution of Cu isotope values with magmatic differentiation. The authors related this evolution to either fractionation during distillation of the Cu from an underlying source or to fractionation within the evolving hydrothermal fluid. However, despite obvious clustering of the  $\delta^{65}\text{Cu}$  values of single intrusions within the composite complex investigated by Graham et al. (2004), which allows tracing the evolution of copper isotope values with time and differentiation, there is still considerable overlap of the data among various intrusions effectively preventing a single analysis being related to a specific source. Furthermore, their data stem from a relatively small group of samples which renders their interpretation more difficult.

Based on ion-exchange experiments at room temperature, Marechal and Albarede (2002) argued for equilibrium

ion-exchange fractionation in aqueous solutions and reject the possibility of a significant effect resulting from the presence of various coexisting oxidation states. Riuz et al. (2002) relates experimentally observed variations to the control of a solid copper phase, which is in equilibrium with a low-temperature fluid. O’Nions and Zhu (2002) and Zhu et al. (2002), however, observed a dependence of isotope fractionation on redox reactions and various oxidation states of copper. Consequently, the mechanism of low-temperature isotope fractionation in aquatic systems is still a matter of debate. However, as isotopic variation especially in these systems is large ( $6\%$  in natural malachite according to Marechal and Sheppard, 2002), it is of interest to study these processes in greater detail.

Here, we report Cu isotope ratios determined for 79 samples of various copper minerals from hydrothermal deposits in a well-investigated mining district of Central Europe, the Schwarzwald in Southwest Germany. The purpose of this study was (1) to investigate the isotopic variability of primary and secondary copper minerals in a large, geologically diverse mining district formed over a period of 300 Million years and (2) to relate measured copper isotope variations to petrographically observed changes in mineralogy of a sample at a specific sample location. As the geological and geochemical background of this mining district is very well understood (Metz et al., 1957; Werner and Franzke, 1994; Werner et al., 2000; Schwinn and Markl, 2005; Schwinn et al., 2006; Markl et al., in press), this area appears to be particularly suited for such a study.

## 2. Geological context, samples and sample locations

The Variscan gneissic and granitic basement in the Schwarzwald area, Southwest Germany, is bounded to the West by the Tertiary Rhinegraben structure and is overlain to the East by partly eroded relics of Mesozoic sedimentary sand- and limestones (which are locally called Buntsandstein (sandstones) and Muschelkalk (limestones)). The ortho- and paragneisses of the basement were intruded by granitoid plutons around  $335$ – $315$  Ma (Kalt et al., 2000). The crystalline rocks show abundant secondary alteration, with chloritization of biotite and sericitization and albitization of feldspars being the most notable alteration features. Oxygen isotope investigations of Hoefs and Emmermann (1983) and Simon and Hoefs (1987) indicate the interaction of the basement with a meteoric fluid at temperatures below  $500\text{ }^\circ\text{C}$ . This alteration event has been dated by K–Ar and Ar–Ar studies of sericitized feldspars from the basement and the overlying Triassic sandstone (Buntsandstein) at  $150$ – $110$  Ma (Zuther and Brockamp, 1988; Lippolt and Kirsch, 1994; Meyer et al., 2000).

The Schwarzwald basement and the Triassic Buntsandstein host a large number of hydrothermal vein-type deposits. Within an area of  $100$  by  $50$  km, more than  $400$  individual veins are known. Most of these veins are sub-economic, but they have been mined for Ag, Pb, Zn, Co,

U or Cu since Roman times. In one deposit (Clara mine near Wolfach, 2 km West of no. 11 on Fig. 1), a barite–fluorite vein is still actively exploited. Several hydrothermal events can be recognized by their distinctive mineralogy, including, for example, Sb–Ag-bearing quartz-veins (occurring throughout the entire district), Co–Ni–Ag–Bi–U-bearing barite–fluorite-veins (in the Wittichen area, number 12–13 on Fig. 1), Fe–Mn-bearing quartz–barite-veins (in the Eisenbach area to the NE of Neustadt on Fig. 1), Cu–Bi-dominated quartz–barite veins in the area between Freudenstadt and Neubulach in the northern Schwarzwald (number 4, q2 and 64 in Fig. 1) or the Pb–Zn–(Ag)-bearing quartz–fluorite-assemblages in the southern Schwarzwald (Metz et al., 1957; Bliedtner and Martin, 1986).

Based on observed structures, fluid inclusion studies (Baatartsogt et al., in press) and by comparison with veins

from the Rheinisches Schiefergebirge (Rhenish Massif; Wagner and Cook, 2000) in Central Germany, the hydrothermal deposits of the Schwarzwald area have been classified into Variscan Sb–(±Ag ± Bi)–quartz veins and post-Variscan fluorite–barite–quartz veins. Most of the post-Variscan veins do not host minerals suitable for radiometric dating. For some of these veins such as Badenweiler, however, a Tertiary age is proven by their occurrence on the Tertiary Rhinegraben boundary fault (Schwarzwald–Randverwerfung). Radiometric datings of pitchblende (U–Pb and U–Xe, Xe–Xe), hematite (U–He), and K-bearing minerals (K–Ar) from other veins revealed the presence of at least three mineralization events: (1) at the end of the Variscan orogeny (310–280 Ma; Wittichen area, Menzenschwand deposit; Hofmann and Eikenberg, 1991; Meshik et al., 2000), (2) at 150–110 Ma (Hohberg and

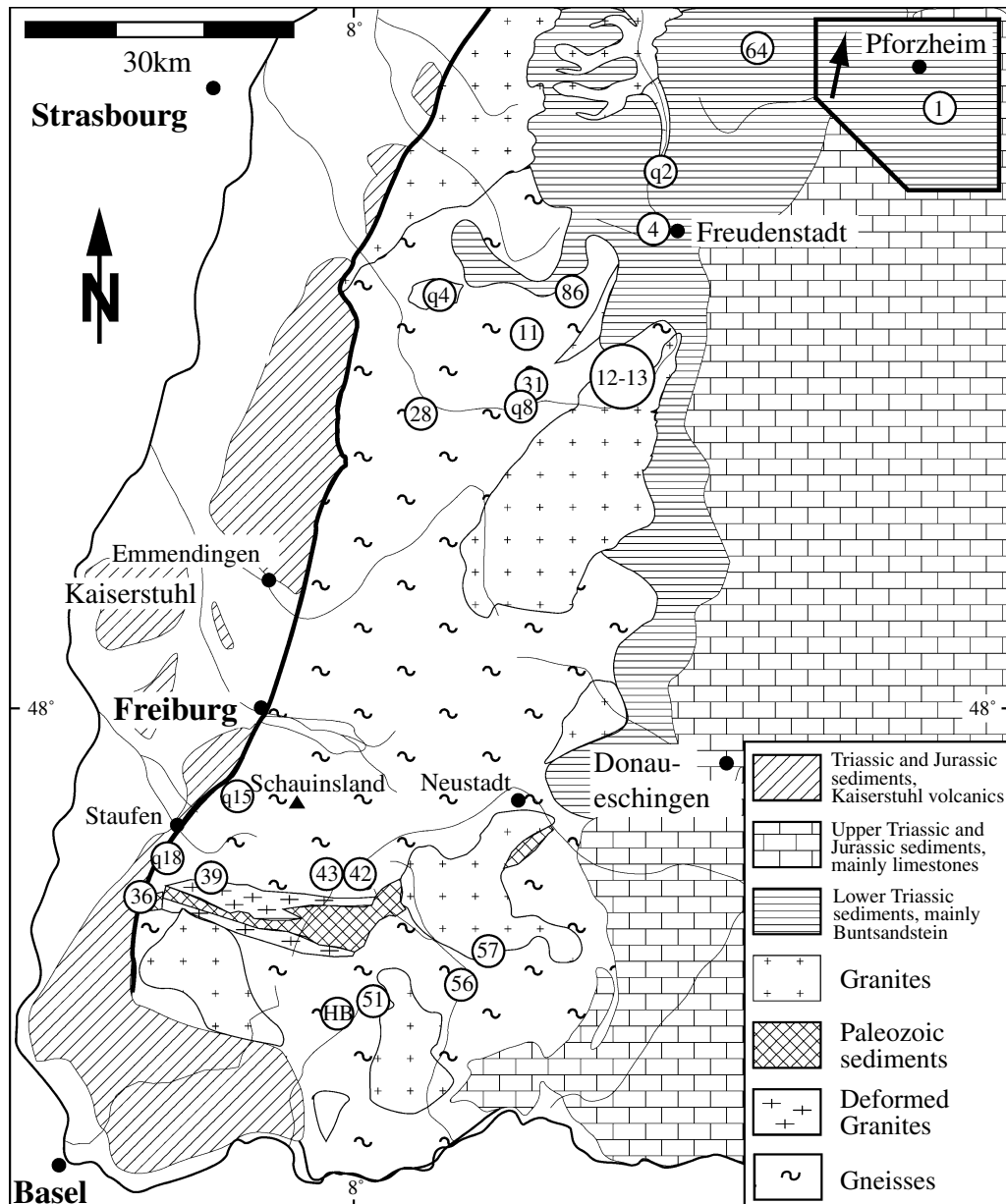


Fig. 1. Simplified geological map of the Schwarzwald area, Southwest Germany, with the sample locations of this study (see also Table 1).

Eisenbach area; Segev et al., 1991; Wernicke and Lippolt, 1994; Wernicke and Lippolt, 1997), and (3) at 50–30 Ma related to the formation of the Rheingraben structure (Menzenschwand deposit; Hofmann and Eikenberg, 1991). Fluid-rock interaction with alteration of primary micas and feldspars to secondary chlorite and clay minerals is believed to have mobilized large amounts of the elements now concentrated in the Mesozoic and Tertiary veins (Schwinn and Markl, 2005). Hence, the source of e.g. the Ba, F, Ag, U and Cu in the hydrothermal deposits are most probably the Variscan gneisses and granites.

The samples of the present study originate from all principal types of mineralizations described above which host at least small amounts of copper minerals. These include the Variscan quartz veins, the Ag–Bi–U–Co-bearing barite–quartz–fluorite veins from Wittichen, the Cu–Bi–quartz-veins from the northern Schwarzwald, and the Pb–Zn-dominated barite–fluorite veins from the southern Schwarzwald. Some minor deposits have been classified separately (see Metz et al., 1957). In addition, a chalcopyrite sample from a magmatic Fe–Ni–Cu deposit in a norite body near Horbach in the Southern Schwarzwald was sampled. The sample locations are shown on Fig. 1 and the samples are briefly described in Table 1. It was the aim of the sampling strategy to cover

- (a) a large variety of different types of veins in the Schwarzwald area to identify primary differences in copper isotope compositions,
- (b) the whole area of the Schwarzwald (about 100 by 50 km) in order to identify potential regional variations, and
- (c) many different primary and secondary copper minerals containing copper in different valence states, where possible from the same deposit, to identify any variations of copper isotope compositions due to oxidation state or redox reactions.

Primary copper ores include chalcopyrite, fahlore (tennantite–tetrahedrite) and emplectite, which all contain essentially Cu(I). These primary ores reacted to secondary copper minerals which include native copper (Cu(0)), cuprite (Cu(I)) and chalcocite (Cu(I)) at two deposits and Cu(II) minerals such as malachite, azurite, olivenite, pseudomalachite, tenorite or chrysocolla in most deposits (see Table 1 for mineral formulae). In all samples, the secondary Cu(II) minerals formed at the expense of one of the three above-mentioned primary ore minerals during interaction with low-temperature (<50 °C) oxidizing solutions. This may have happened directly on the surface of the primary ores or the secondary minerals formed in cavities close to the primary ores (some centimeters to few decimeters away from the primary ore). Obviously, the copper was transported to the site of growth by the oxidizing solution. Low temperatures for this process are proved by our observation, that at least some of the secondary minerals form in old mine workings and dumps.

If different minerals in Table 1 have the same sample numbers, they were hand-picked from the same sample. Typically, they were sampled only millimeters to a few centimeters away from each other in order to check for local fractionation processes on the hand-sample scale. Samples without any signs of secondary copper minerals under the binocular microscope were considered “fresh” and it is these samples which are interpreted to record the primary copper isotope composition of the high-temperature mineralizing fluids (about 120–200 °C; Schwinn et al., 2006).

Cuprite, native copper and chalcocite formed at one deposit (Rippoldsau, see Table 1) at the expense of chalcopyrite under comparatively reducing, low-temperature conditions. At this locality, some samples of chalcopyrite are completely replaced by an intimate intergrowth of native copper and cuprite, which is in turn overgrown by later malachite. At Neubulach, native copper texturally appears to replace azurite which in turn had formed from the decomposition of fahlore. The same appears to be true for cuprite from Neubulach, although the textural interpretation is ambiguous.

In summary, this study combines samples from the whole area of the Schwarzwald and from different types of veins which all together span almost 300 Ma of formation history. The samples record the effects of low-temperature redox processes on the copper isotope compositions of primary higher temperature, hydrothermal copper ores.

### 3. Analytical methodology

#### 3.1. Sample preparation

Cu-rich mineral grains of 0.5–2 mm size were hand-picked and appeared clean during examination under a binocular microscope. These grains were dissolved in few milliliters of aqua regia, which was successively evaporated at a temperature of about 40 °C overnight. All samples analyzed without chromatography were dissolved in 2% HNO<sub>3</sub> to yield a final concentration of about 500 ppb Cu. Some samples were prepared for chromatography and were dissolved in 6 N HCl in a 5 ml Savillex beaker, then purified in a single-pass HBr-based anion resin (Dowex 1\*8, 100–200 mesh) separation and subsequently converted to nitrate.

This standard anion-exchange procedure for chemical separation and purification is modified from Manhés et al. (1978). All the diluted samples were spiked with 1 ppm of the Ni standard NIST SRM-986 of known isotopic composition. A blank measurement was performed at the beginning of the sequences. Samples and standards values were blank corrected although the total blank levels remained below 100 pg and are negligible.

#### 3.2. Internal and external standardization

The certified ratio of 0.1386 for <sup>62</sup>Ni/<sup>60</sup>Ni in the Ni NIST SRM-986 standard was used to correct for the

Table 1  
Samples, sample localities and results of the copper isotope measurements

Mine	No. on Fig. 1	Mineral	Fresh/oxidized	Sample number	$\delta^{65}\text{Cu}$ (in ‰, without ion chromatography) <sup>a</sup>	$\delta^{65}\text{Cu}$ (in ‰, with ion chromatography) <sup>a</sup>	$\delta^{65}\text{Cu}$ (in ‰, without ion chromatography) <sup>b</sup>
Dorothea near Freudenstadt	4	Chalcopyrite	Fresh	M33	-0.78		-0.65
		Fahlore	Fresh	Cu11	0.06	0.04	-0.01
		Fahlore	Oxidized	QDC55	-0.23		-0.36
		Fahlore	Oxidized	QDC32	-0.08		-0.09
		Emplectite	Oxidized	QDC63	-1.49	-1.76	-1.75
		Malachite		QDC8	-0.40	-0.38	-0.39
		Olivenite		QDC38	1.24	1.39	1.26
		Fahlore	Oxidized	QDC20	-1.28		-1.25
		Olivenite		QDC20	2.41		2.42
		Malachite		Cu13	2.33		2.25
Königswart, Baiersbronn	q2	Emplectite	Fresh	Cu6	-0.90		-0.97
		Chalcopyrite	Slightly ox.	Cu5	-1.63	-1.67	-1.64
		Fahlore	Slightly ox.	Cu7	-1.65		-1.72
		Fahlore	Oxidized	Cu8	-2.52		-2.40
		Malachite		Cu8	-0.70		-0.64
Neubulach near Calw	64	Chalcopyrite	Slightly ox.	BTR25	-1.97		-1.95
		Native copper		NNB82	-0.48		-0.46
		Malachite		NNB43	0.13		0.18
		Cuprite		NNB43	1.69		1.67
		Tenorite		Cu9	0.91	0.83	0.89
		ps. a. azurite					
		Azurite		Cu10	-1.55		-1.72
		Fahlore	Oxidized	NNB91	-1.96		-1.93
Malachite		NNB91	-0.36		-0.25		
Prosper near Rippoldsau	86	Chalcopyrite	Fresh, with nat. sulphur	SBR5	0.46		0.34
		Chalcopyrite	Fresh	Cu2	-0.14		-0.35
		Cuprite		Cu14	0.49		0.65
		Malachite		Cu14	1.01		1.04
		Native copper		Cu3	0.36		0.39
		Cuprite		Cu3	0.46		0.45
		Malachite		Cu3	0.82		0.93
		Chalcocite, little chalcop.		SBR2	-1.89		-1.85
Chalcopyrite	Slightly ox.	Cu4	-0.48		-0.39		
Mettmatal near Brenden	56	Chalcopyrite	Fresh	MS1466	-0.09		-0.12
		Chalcopyrite	Fresh	MS33	-0.03		-0.01
		Chalcopyrite	Oxidized		-0.09		-0.04
		Malachite		IBM30	-0.71		-0.64
Baumhalde near Todtnau	42	Malachite	On gneiss	ZBH37	-0.12		-0.04
		Cuprite	On gneiss	ZBH37	0.55		0.64
		Malachite		ZBH36	0.62		0.77
		Chalcopyrite	Fresh	ZBH31	0.08		0.02
Friedrich-Christian near Schapbach	11	Chalcopyrite	Fresh	Std1	-0.01		0.04
		Chalcopyrite	Fresh	Std2	0.14		0.07
		Chalcopyrite	Fresh	Std4	0.00		-0.02
		Chalcopyrite	Fresh	Std5	0.09		0.12
		Chalcopyrite	Fresh	M844	-0.35		-0.32
		Chalcopyrite	Oxidized	M928	-2.27		-2.21
		Chalcopyrite	Oxidized	M2-1	-1.64		-1.60
		Chalcopyrite	Fresh	GS129	-0.12		-0.13
		Chalcopyrite	Fresh	GS135	-0.31		-0.31
		Chalcopyrite	Oxidized	M2-2	-2.92		-2.85
		Malachite		M2-2	1.49		1.52
		Chalcopyrite	Oxidized	Metz57	-0.96		-0.98
Malachite		Metz57	1.01		1.01		

(continued on next page)

Table 1 (continued)

Mine	No. on Fig. 1	Mineral	Fresh/oxidized	Sample number	$\delta^{65}\text{Cu}$ (in ‰, without ion chromatography) <sup>a</sup>	$\delta^{65}\text{Cu}$ (in ‰, with ion chromatography) <sup>a</sup>	$\delta^{65}\text{Cu}$ (in ‰, without ion chromatography) <sup>b</sup>
Gottesehre near Urberg	51	Chalcopyrite	Fresh	M810	-0.15		0.11
		Chalcopyrite	Fresh	Cu1	-0.11		-0.17
		Chalcopyrite	Oxidized	Wein8438	-0.54		-0.47
		Chrysocolla		Wein8438	1.91		1.95
Silberbrünnle, Gengenbach	q4	Chalcopyrite	Slightly ox.	YSB235	-0.35		-0.41
		Malachite		YSB161	1.81		1.82
		Pseudomalachite		YSB115	0.29		0.21
Haus Baden, Badenweiler	36	Malachite with covellite		BHB112	1.12		1.14
		Chalcopyrite	Fresh	BHB116	0.05		0.05
	q8	Chalcopyrite	Oxidized	BTR24	-0.54		-0.54
		Malachite		Lo1	0.95		1.10
Schlüchtal, Igelschlatt	57	Chalcopyrite	Oxidized	IGH20	-0.52		-0.55
		Malachite		IGH22	0.50		0.56
Brandenberg near Todtnau	43	Chalcopyrite	Fresh	GS78	0.13		0.17
		Malachite		Metz392	-0.16		-0.09
Rammelsbach, Münstertal	39	Chalcopyrite	Oxidized	804	-1.93		-1.84
		Malachite		M7	2.04		2.07
Artenberg near Steinach	28	Chalcopyrite	Fresh	BTR13	0.06		0.02
Käfersteige, Pforzheim	1	Chalcopyrite	Fresh	BTR34a	0.01		-0.03
					0.03		
Wenzel near Wolfach	31	Chalcopyrite	Fresh	OWF18	-0.03		0.00
					-0.03		
Sophia near Wittichen	12	Chalcopyrite	Fresh	WSB26	-0.13		-0.11
					-0.14		
Sophia near Wittichen	12	Chalcopyrite	Fresh	WSB181	0.40		0.42
					0.42		
Johann a. B., Wittichen	13	Chalcopyrite	Oxidized	WJB2	-0.62		-0.72
					-0.63		
Friedrich-August near Horbach	HB	Chalcopyrite	Fresh	CuK	0.16		0.17
Birkenberg near St. Ulrich	q15	Chalcopyrite	Fresh	DSU16	0.16		0.12
					0.13		
Holderpfad near Sulzburg	q18	Chalcopyrite	Fresh	DSB39	0.49		0.44
					0.48		

Note that some samples have been measured for comparison using ion exchange chromatography. Various minerals with identical sample numbers indicate that they have been taken from the same hand specimen.

Note: the chemical formulae of the minerals investigated are: chalcopyrite  $\text{CuFeS}_2$ , fahlore  $(\text{Cu,Ag})_{10}(\text{Fe,Zn})_2(\text{As,Sb, Bi})_4\text{S}_{13}$ , malachite  $\text{Cu}_2\text{CO}_3(\text{OH})_2$ , azurite  $\text{Cu}_3(\text{CO}_3)_2(\text{OH})_2$ , covellite  $\text{CuS}$ , chalcocite,  $\text{Cu}_2\text{S}$ , emplectite  $\text{CuBiS}_2$ , pseudomalachite  $\text{Cu}_5(\text{PO}_4)_2(\text{OH})_4$ , chrysocolla  $\text{Cu}_2\text{H}_2\text{Si}_2\text{O}_5(\text{OH})_4 \cdot n\text{H}_2\text{O}$ , cuprite  $\text{Cu}_2\text{O}$ , tenorite  $\text{CuO}$ , native copper  $\text{Cu}$ , olivenite  $\text{Cu}_2\text{AsO}_4\text{OH}$ .

<sup>a</sup> Mass bias corrected using the Ni standard NIST SRM-986.

<sup>b</sup> Mass bias corrected using NIST SRM-976 by standard bracketing.

mass bias of the Cu isotopes using an exponential law of mass discrimination. The  $\delta^{65}\text{Cu}$  values were obtained after normalization to the Ni NIST SRM-976 standard measured during the same analytical session. The potential difference of instrumental mass fractionation between the Cu NIST SRM-976 and Ni NIST SRM-986 standards has been evaluated. The Cu NIST SRM-976 standard and two samples have been analyzed five times after being mixed with the Ni NIST SRM-986 standard. The results are presented in Table 2 and on Fig. 2. The excellent correlation and the slope of 1 observed between  $\ln(^{63}\text{Cu}/^{65}\text{Cu})$  and  $\ln(^{60}\text{Ni}/^{62}\text{Ni})$  shows that Ni could be used as an internal standard for Cu isotope measurements. The standard NIST SRM-976 was used to

monitor the precision of the measurements over the whole period of analysis and was analyzed after every second sample analysis. Table 1 compares the  $\delta^{65}\text{Cu}$  values calculated using the Ni NIST SRM-986 standard as an internal standard or using the Cu NIST SRM-976 standard for external standard bracketing. The  $\delta^{65}\text{Cu}$  values differ on average less than 0.06‰ between the two normalization techniques.

### 3.3. Repeatability of $^{65}\text{Cu}/^{63}\text{Cu}$ measurements

Table 2 also shows the results of duplicate measurements of two samples (BTR25 and M33) and shows an external reproducibility of 40 ppm or 0.04‰ ( $2\sigma$ ) using

Table 2

Results of repeated measurements of the copper isotope compositions with NIST 986 addition in the Cu NIST976 standard and two samples

	$R^2$	$n$	$^{65}\text{Cu}/^{63}\text{Cu}$	$2\sigma$	$^{62}\text{Ni}/^{60}\text{Ni}$	$2\sigma$	$\delta^{65}\text{Cu}$ (‰)	$2\sigma$
NIST SRM-976–NIST SRM-986 mixture	0.99	11	0.47460	0.00026	0.147877	0.000081		
BTR 25	0.98	5	0.47336	0.00035	0.147778	0.000108	−2.00	0.04
M33	0.98	5	0.47391	0.00028	0.147770	0.000089	−0.76	0.04

$n$ , number of analyzes;  $R^2$ , correlation coefficient.

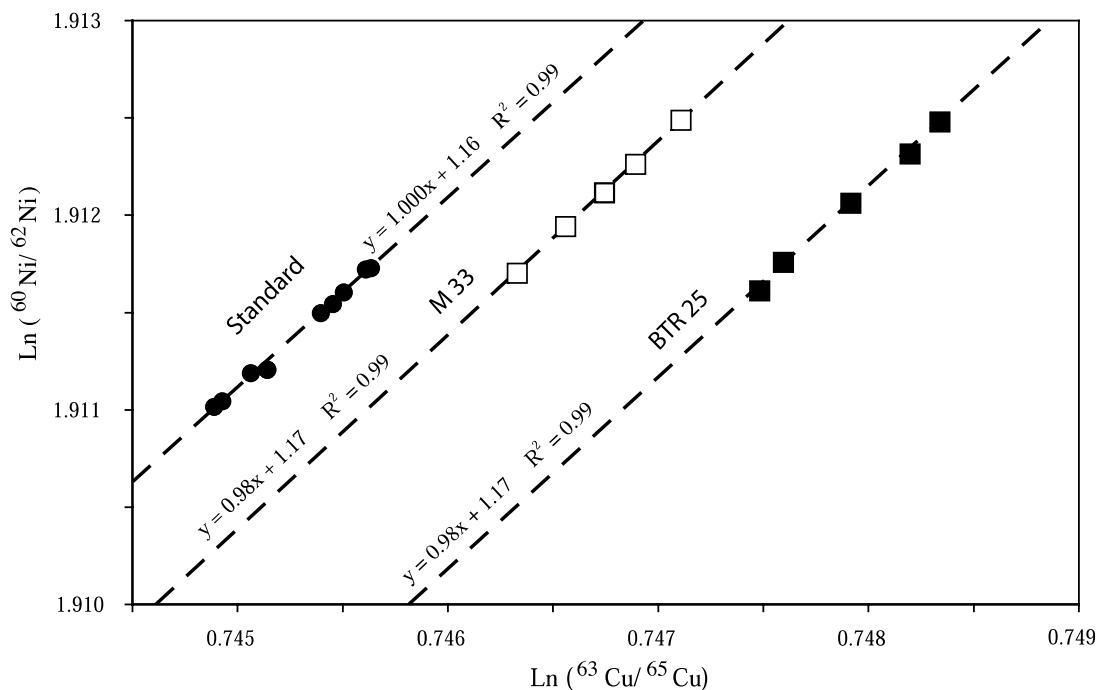


Fig. 2.  $\ln(^{63}\text{Cu}/^{65}\text{Cu})$  vs.  $\ln(^{60}\text{Ni}/^{62}\text{Ni})$  plot of the raw ratios of mixed Cu NIST SRM-976 standard and two samples (samples 24 and 29) mixed with Ni NIST SRM-986.

Ni as an internal standard for mass bias correction. Other duplicate samples are shown in Table 1 using the same normalization technique and the calculated  $\delta^{65}\text{Cu}$  values are on average within 0.02‰.

### 3.4. Chromatographic separation

The effect of ion-exchange chromatography has been evaluated by comparing the calculated isotope ratios from the same samples that were simply digested and diluted and those purified by chromatography prior to mass spectrometry. A variety of copper minerals, which cover the entire range of mineral compositions studied here (fahlore  $(\text{Cu}, \text{Ag})_{10}(\text{Fe}, \text{Zn})_2(\text{As}, \text{Sb}, \text{Bi})_4\text{S}_{13}$ , emplectite  $\text{CuBiS}_2$ , malachite  $\text{Cu}_2\text{CO}_3(\text{OH})_2$ , olivenite  $\text{Cu}_2\text{AsO}_4\text{OH}$ , azurite  $\text{Cu}_3(\text{CO}_3)_2(\text{OH})_2$  and chacopyrite  $\text{CuFeS}_2$ ) have been selected for this test in order to evaluate the potential matrix effect on the Cu isotope measurements with or without chromatography. The results are presented in Table 1. There is very good agreement between the two sets of data and the results vary on average less than 0.1‰. This variation is at least twice the external reproducibility measured on the standard (0.04‰) and could be due to sample hetero-

ogeneities or to a matrix effect from other elements in the unpurified samples. The emplectite sample QDC63 shows a maximum difference between the two measurements (0.27‰). This difference possibly reflects matrix effects or interferences related to the particularly high concentration of Bi in the emplectite. However, the external reproducibility on the samples is negligible relative to the overall isotopic variation observed in the present study. The effect of the matrix on the accuracy of the results is therefore negligible—with the one possible exception of the emplectite. The absence of a matrix effect on the accuracy of the Cu isotopes analyses using MC-ICP-MS is in agreement with the results of Zhu et al. (2000) and Graham et al. (2004).

### 3.5. Data acquisition

Isotope ratios were determined using a Multi-Collector Inductively Coupled Plasma Mass Spectrometer (Neptune™, Finnigan MAT) at Frankfurt University, Germany, at low resolution ( $\Delta m/m = 400$ ) using five blocks of five integrations of approximately 8.4 s each. Runs of sample and standard were separated by washes using 2%  $\text{HNO}_3$  for 2 min. A 40 s baseline was also systematically acquired

before every measurement. The sample was nebulized into a cyclonic spray chamber using a 50  $\mu\text{l}$  PFA MicroFlow™ nebulizer. An optimal Cu ion current of 3–4 V was achieved on  $^{63}\text{Cu}$  using a 500 ppb solution of Cu.

#### 4. Results

The results of this study are listed in Table 1 and displayed on Fig. 3–5. The  $\delta^{65}\text{Cu}$  values vary over almost 6‰ from  $-3.0$  to  $2.5$ ‰ (Figs. 3 and 4). Despite some minor variations, three features are immediately obvious:

1. Fresh samples of most primary copper ores without any sign of oxidation in the whole specimen cluster in a narrow range around a  $\delta^{65}\text{Cu}$  of  $0 \pm 0.5$ ‰ (25 samples, Fig. 5). Only the two Cu–Bi–quartz deposits of Königswart and Neubulach in the northern Schwarzwald appear to have lower primary  $\delta^{65}\text{Cu}$  values below  $-0.9$ ‰, although from Neubulach it proved to be impossible to find a sample without any sign of oxidation. An absolutely fresh emplectite from Königswart, however, has a value of  $-0.9$ ‰, and only slightly oxidized chalcopyrite and fahlore from this locality have values around  $-1.65$ ‰. The sample BTR25 from Neubulach shows only very minor signs of alteration and no visible alteration of the chalcopyrite grain taken for analysis. Its  $\delta^{65}\text{Cu}$  value is  $-1.97$ ‰. To rule out any analytical artefact, this measurement has been duplicated by selecting it for the additional internal standardization test using Ni standard NIST SRM-986 (Table 2). The strongly negative  $\delta^{65}\text{Cu}$  values from these two localities were taken as indication of a light primary  $\delta^{65}\text{Cu}$  value. The magmatic chalcopyrite sample from Horbach is isotopically indistinguishable from the hydrothermal vein-type mineralizations. Within multiply mineralized single deposits, no systematic variations of Cu isotope compositions with paragenesis or different generations were observed. It is also important to note, that the two “anomalous” deposits do not differ from the other

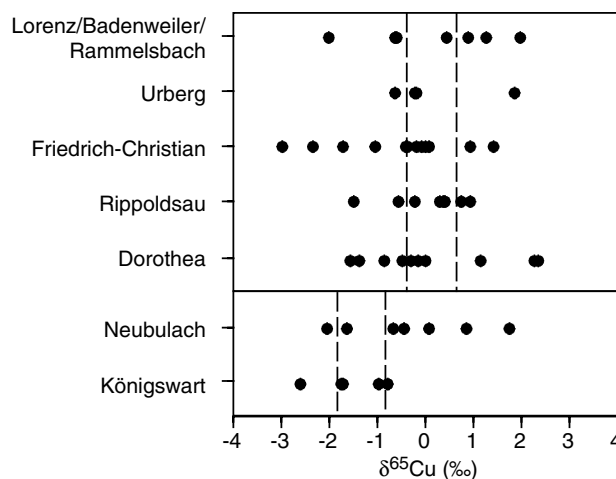


Fig. 4. Copper isotope compositions of various copper minerals from selected localities in the Schwarzwald mining district. Note the large spread in  $\delta^{65}\text{Cu}$  at each locality. The vertical dashed lines indicate the range of copper isotope compositions of fresh, unoxidized primary ores from the localities and show the difference between the two sample groups discussed in the text.

- deposits in terms of their fluid inclusion characteristics (i.e., homogenization temperatures between 150 and 250 °C, salinities between 15 and 25 wt% NaCl equiv.; Baatartsogt et al., in press). In general, no correlation between fluid inclusion characteristics and Cu isotope compositions were observed.
2. Cu(I) minerals generally have lower  $\delta^{65}\text{Cu}$  values than Cu(II) minerals (Fig. 3). No primary Cu(I) mineral has a  $\delta^{65}\text{Cu}$  value above  $0.6$ ‰, no Cu(II) mineral has a  $\delta^{65}\text{Cu}$  value below  $-1.55$ ‰. Native copper has values between  $-0.5$  and  $0.4$ ‰.
3. While the primary  $\delta^{65}\text{Cu}$  values of fresh ores do not vary significantly (apart from Königswart and Neubulach, see bullet point 1 above), altered samples may show differences of up to  $4$ ‰ in a specific deposit and up to  $3$ ‰ in a specific mineral (Fig. 5). Supergene

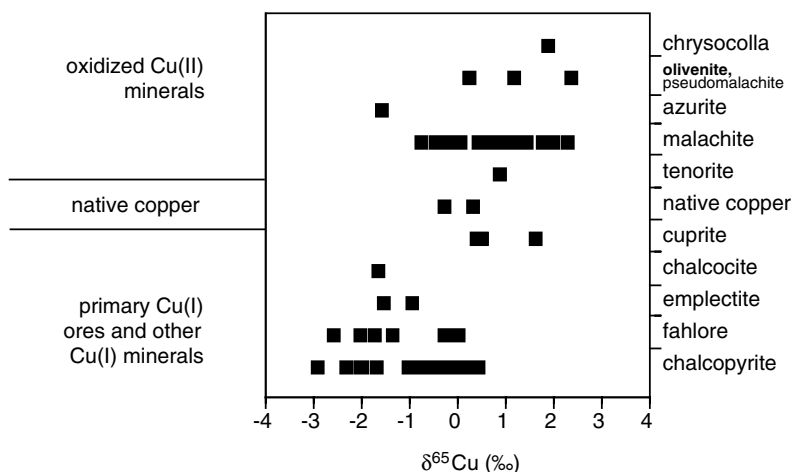


Fig. 3.  $\delta^{65}\text{Cu}$  values for all analyzed samples from the Schwarzwald mining district.

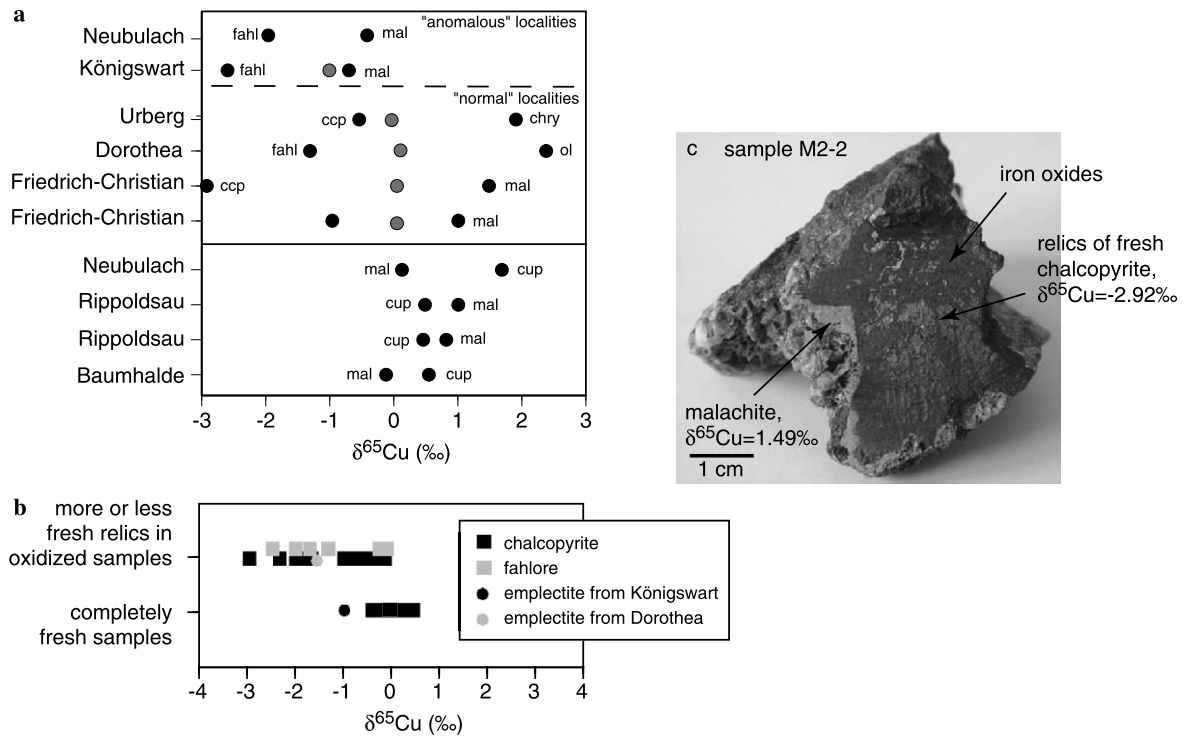


Fig. 5. (a)  $\delta^{65}\text{Cu}$  of minerals from the same hand specimen. The diagram is divided into three parts: the uppermost part shows secondary Cu(II) minerals in contact with relics of primary Cu(I) minerals from the two “anomalous” localities, where the fresh, primary Cu(I) minerals appear to have  $\delta^{65}\text{Cu}$  values significantly different from 0; the middle part shows secondary Cu(II) minerals in contact with relics of primary Cu(I) minerals from localities where the fresh, primary Cu(I) minerals have  $\delta^{65}\text{Cu}$  values around 0; the lowermost part shows secondary Cu(II) minerals in contact with relics of secondary Cu(I) minerals (cuprite). The grey symbols indicate the  $\delta^{65}\text{Cu}$  values of fresh, primary Cu(I) minerals from the respective locality. Note, that no fresh sample could be measured from Neubulach. (b)  $\delta^{65}\text{Cu}$  values of Cu(I) ore minerals (chalcopyrite, fahllore and emplectite). Completely fresh samples cluster in a narrow range around 0‰ (note, however, that the fresh emplectite from Königswart is significantly lighter!), whereas partly oxidized samples exhibit a range of  $\delta^{65}\text{Cu}$  values down to  $-3\text{‰}$ . (c) Photograph of sample M2-2 from the Friedrich-Christian mine in Wildschapbach. The particles analyzed (Tables 1 and 2) were taken from about the areas, where the “malachite” and the “chalcopyrite” arrows point. Abbreviations: fahl, fahllore; cup, cuprite; mal, malachite; chry, chrysocolla; ol, olivenite; ccp, chalcopyrite.

Cu(II) minerals become isotopically heavier, while the relics of the primary Cu(I) mineral become isotopically lighter (Fig. 5). In some samples, this observation appears to be correlated to the extent of reaction (i.e., the more of a Cu(I) mineral that has macroscopically visible reacted away, the lighter the relict Cu(I) mineral is). In other samples, however, this relation does not hold, and even only slightly oxidized Cu(I) mineral grains have strongly negative  $\delta^{65}\text{Cu}$  values. It appears possible that we were unable to separate the altered and the pristine part of the reacting minerals because of the small-scale mineralogical variation which may have resulted in mixed analyses in some cases.

## 5. Discussion

### 5.1. Source of the copper

Primary  $\delta^{65}\text{Cu}$  values (i.e., from unoxidized, primary, high-temperature hydrothermal minerals) from most copper-bearing mineralizations in the Schwarzwald area (with two exceptions discussed below) tightly cluster in the range

$0 \pm 0.5\text{‰}$ . This indicates that the primary Cu(I) minerals were precipitated from isotopically relatively homogeneous fluids. Temporal, chemical and regional variations of mineralizations apparently did not play a major role in controlling copper isotope compositions. Furthermore, the small variability of the values indicates that at hydrothermal temperatures of 150–300 °C, fractionation of the Cu isotopes is approximately constant during leaching reactions in the source rocks and during the actual precipitation process, as no systematic variations between fluid inclusion homogenization temperatures and Cu isotope compositions could be observed. This is in contrast to the behaviour of Fe isotopes from the Schwarzwald hydrothermal mineralizations (Markl et al., in press).

However, not all deposits contain primary minerals that conform to the “homogeneous” fluid model. Fahllore and emplectite at Königswart and Neubulach occur in very similar quartz veins with minor barite, while chalcopyrite is rare. Furthermore, these two vein systems are geographically close to each other and hosted by Triassic sandstone (Buntsandstein, Fig. 1). In comparison, two other sandstone-hosted vein deposits within the same area, Käfersteige and Dorothea, that contain vein assemblages dominated by barite and fluorite, do not show this shift

to lighter  $\delta^{65}\text{Cu}$  values in their primary ores. All four deposits (Königswart, Neubulach, Käfersteige and Dorothea) have similar fluid inclusion homogenization temperatures around 150–200 °C (Baatartsogt et al., *in press*). We suggest that the Cu present in Neubulach and Königswart may have precipitated from fluids that contained Cu originating from older copper ores, as oxidation and dissolution of Cu minerals tends to preferentially remove  $^{65}\text{Cu}$  (Rouxel et al., 2004 and this study). As the Schwarzwald basement contains Cu mineralizations with ages between 300 and approximately 20 Ma, it seems likely that remobilization of older copper ores could have occurred during a later hydrothermal event. We consider it surprising that we did not find more indications of such remobilization processes in the course of our study.

Concerning the source of the copper in the hydrothermal solutions, one can only use indirect evidence. Lüders (1994) proposed that the hydrothermal mineralizations formed from the mixing of two fluids: a high-temperature highly saline brine from the basement and meteoric water. Based on fluid inclusion, carbon and sulfur isotope studies, Schwinn et al. (2006) show that the mixing ratios of high- to low-temperature fluid were between 0.7 and 0.5. Furthermore, Schwinn and Markl (2005) suggest that the REE patterns of basement brines reflect intense reactions with the basement gneisses and granites. It appears probable that the metals within these brines were also derived from the basement. These fluid inclusion, C and S isotope and trace element data also suggest that the fluids, from which the vein mineralizations precipitated, were geochemically similar over the entire Schwarzwald region through space and time. The present Cu isotope study generally supports this conclusion. Most probably, the Cu was leached from the basement rocks; if their Cu isotopic composition was variable before, it was homogenized in the course of this process.

### 5.2. Effects of redox reactions on $\delta^{65}\text{Cu}$ values

Both experiments and calculations indicate that in principle, Cu solubility in aqueous fluids increases with falling pressure, rising temperature, decreasing pH, increasing chlorinity and increasing  $f_{\text{O}_2}$ , and that at temperatures above about 120 °C and  $a_{\text{Cl}^-}$  above about 1, highly charged chloro-complexes like  $\text{CuCl}_5^{3-}$  or  $\text{CuCl}_4^{2-}$  are the dominant aqueous copper species in relatively oxidized solutions (Seyfried and Ding, 1993; Xiao et al., 1998; Collings et al., 2000; Brugger et al., 2001; Liu et al., 2001; Mountain and Seward, 2003). At lower temperatures and chlorinities, either  $\text{CuCl}^0$  or sulphide complexes are of increasing importance. Brugger et al. (2001) could show that in low-temperature fluids at 25 °C, Cu(II) becomes dominant at  $f_{\text{O}_2}$  values above  $10^{-25}$  to  $10^{-35}$ , depending on the chlorinity of the fluid. As we assume that the low-temperature fluid is in equilibrium with air, it is obvious that a Cu(II) species, and most probably  $\text{CuCl}_2(\text{aq})$  or  $\text{CuCl}^+(\text{aq})$  at a  $\text{Cl}^-$  activity around  $10^{0.5}$  is the dominant species during

the weathering reactions. The high-temperature mineralization, in contrast, most probably crystallized from a relatively reduced and much more saline brine (Schwinn et al., 2006; Baatartsogt et al., *in press*), in which a highly charged chlorocomplex was the dominant copper species. For our discussion at present it is important to note, that the high-temperature Cu(I) minerals stably formed from a Cu(I)-dominated brine, while the low-temperature alteration assemblage of Cu(II) phases are in equilibrium with a Cu(II)-dominated solution. While influx of oxidizing fluids not in equilibrium with the chalcopyrite was the reason for dissolution, most probably a pH increase due to fluid–rock interaction was responsible for reprecipitation of the dissolved copper as malachite or another Cu(II) mineral. In the case of the formation of a secondary Cu(I) or Cu(0) mineral, the weathering fluid may have been not in equilibrium with air, but may have contained reducing species such as methane or other organic compounds related to degrading organic material close to the surface.

It is obvious that low-temperature alteration seriously affected the copper isotope composition of Schwarzwald copper minerals (Fig. 5), which is in agreement with previous studies (Zhu et al., 2000, 2002; Marechal and Sheppard, 2002; O’Nions and Zhu, 2002; Riuz et al., 2002; Rouxel et al., 2004). Rouxel et al. (2004) found that low-temperature alteration of sulfides from hydrothermal seafloor vents produces secondary copper minerals enriched in  $^{65}\text{Cu}$ , whereas the actual high-temperature precipitation process did not lead to variations in  $\delta^{65}\text{Cu}$ .

The depletion of the lighter isotope  $^{63}\text{Cu}$  in the Cu(II) minerals during the oxidation of the primary copper ores can be explained in two ways: either, the heavier isotope  $^{65}\text{Cu}$  reacts more strongly than the lighter isotope  $^{63}\text{Cu}$ , or, both isotopes are oxidized similarly, but the heavier isotope is preferentially incorporated into the solid Cu(II) phase. This means the fractionation could be controlled either by the redox/dissolution or by the precipitation step. Based on the simultaneous change to lighter  $\delta^{65}\text{Cu}$  values of the chalcopyrite, fahlore and emplectite during the redox process, it appears most probable that the redox process controls the isotope fractionation, as the increased amount of  $^{65}\text{Cu}$  in secondary Cu(II) minerals is balanced by lighter  $\delta^{65}\text{Cu}$  values in the remaining Cu(I) without any sign of any newly precipitated Cu(I) mineral which could change the bulk  $\delta^{65}\text{Cu}$  value.

It appears that on a cm-scale the alteration proceeds in a closed system with respect to the copper isotopes. This, in turn, would require, that solid-state diffusion within the Cu(I) ores during low temperatures is fast enough to enable diffusion of  $^{65}\text{Cu}$  through the sulfide towards the reaction site even over a distance of some millimeters, or that dissolution and reprecipitation occurs on a very small scale. It is important to note that both processes mentioned above could involve equilibrium fractionation or they could be kinetically controlled, e.g., by different rate constants for the dissolution and/or precipitation of Cu(I) and Cu(II). At present, we cannot decide between the two alternatives,

although a rate-controlling (i.e. kinetic) process is less likely because in our samples, the heavier isotope more readily reacts (which is contrary to what one would expect in a kinetic process).

A comparison with published fractionation factors (fractionation factor in a copper-bearing solution:  $\alpha_{\text{Cu(II) species/Cu(I) species}} = (^{65}\text{Cu}/^{63}\text{Cu})_{\text{Cu(II) species}} / (^{65}\text{Cu}/^{63}\text{Cu})_{\text{Cu(I) species}}$ ) in low-temperature experimental systems shows good agreement between our natural findings and these experiments. Zhu et al. (2002) published fractionation factors between 1.00394 and 1.00412 for Cu(II)/Cu(I) in aqueous nitrate solutions at room temperature, in which Cu(II) nitrate was reduced and precipitated as Cu(I) iodide. The authors state that fractionation can occur either during the redox reaction in solution or during the precipitation of the salt. However, due to the small solubility product of Cu(I), they assume that the redox reaction is mainly responsible for the copper isotope fractionation. Ehrlich et al. (2005) measured Cu isotope fractionation between CuS (covellite) and aqueous Cu(II) solution and found a mean fractionation of  $3.16 \pm 0.14\%$  between Cu(II) solution and solid CuS with an inverse temperature dependence. Unfortunately, both the Zhu et al. (2002) and the Ehrlich et al. (2005) experiments could not completely rule out kinetic fractionation effects. Hence, kinetic vs. equilibrium effects in these experiments are unclear and isotopically heavy Cu(II)-minerals could be the result of partial reduction of Cu(II) to secondary Cu(I).

Marechal and Sheppard (2002) performed experiments at 30 and 50 °C, in which they synthesized malachite from a Cu(II) solution by reaction with calcite. Hence, no redox process was involved in these experiments. They found that fractionation occurred, but fractionation factors between solution and mineral were an order of magnitude smaller than during the redox process and ranged between 1.00020 and 1.00038 at 30 °C and between 1.00017 and 1.00031 at 50 °C. This may indicate that rising temperature reduces the fractionation.

Comparison of these two experimental studies with each other and with our results from natural samples support the interpretation that the large observed natural variation cannot be accounted for by solid-fluid equilibrium fractionation alone, but that redox processes have by far the largest effect on copper isotope variations. While in the experiments of Zhu et al. (2002), reduction in solution produced the fractionation, we observed the largest effects during oxidation from Cu(I) to Cu(II). Reduction of Cu(II) to Cu(0) or Cu(I) to Cu(0) did not appear to have a similarly large effect, as native copper has  $\delta^{65}\text{Cu}$  values similar to its precursor minerals. We interpret this discrepancy to result from the combination of solid-fluid (i.e., between fluid and mineral) and within-fluid fractionation (i.e., between Cu(I) and Cu(II) ions), although the detailed underlying mechanism remains unclear.

The calculation of a bulk fractionation factor Cu(II)-mineral/Cu(I)-mineral appears hindered by the fact that both values of the secondary and of the primary minerals

show large variations even within one sample. However, if one defines a fractionation factor  $\alpha$  as

$$\alpha_{\text{Cu(II)mineral/Cu(I)mineral}} = (^{65}\text{Cu}/^{63}\text{Cu})_{\text{Cu(II)mineral}} / (^{65}\text{Cu}/^{63}\text{Cu})_{\text{Cu(I)mineral}}$$

and combines the copper isotope values of Cu(II)–Cu(I) mineral pairs taken from the same sample, then  $\alpha$  values between 0.9984 and 1.004 are calculated (Table 3). This is almost exactly the range observed in the experiments by Marechal and Sheppard (2002) and by Zhu et al. (2002). More interesting, however, is the observation that fractionation factors between secondary Cu(II) and primary Cu(I) minerals range between 1.0016 and 1.0044 (first group in Table 3) and that they are significantly different from fractionation factors between secondary Cu(II) and secondary Cu(I) minerals, which range between 0.9984 and 1.0005 (second group in Table 3). Texturally, the secondary Cu(I) mineral in the second group of samples formed from a primary Cu(I) mineral (chalcopyrite or fahlore, no relics left today), before the secondary Cu(II) mineral on the respective sample formed. These values could be interpreted as reflecting fluid–solid and within–fluid equilibrium, respectively, for which the experiments cited above indicate values of 1.0002 (fluid–solid) and 1.0040 (within–fluid). However, it is not clear why the direct oxidation of a primary Cu(I) mineral should have an effect different from the oxidation of a secondary Cu(I) mineral.

As the experimental results indicate that fractionation factors between aqueous Cu(I) and aqueous Cu(II) are larger relative to fractionation between aqueous Cu(I) and solid Cu(II), this may indicate different mechanisms of secondary mineralization. In the one scenario the primary ore is oxidized by low-temperature fluids, and the Cu(II) in the oxidized fluid is precipitated as secondary Cu(II) mineral. In the second scenario, the low temperature fluid contains a mix of Cu(I) and Cu(II), the Cu(I) minerals precipitate first, and as the fluid evolves and becomes more oxidizing, the Cu(II) precipitates, reflecting the large fluid–fluid fractionation factor. Fig. 6 shows the fractionation effect of mass balance in Rayleigh-type calculations in a

Table 3  
Fractionation factors calculated for mineral pairs sampled on the same specimen

Sample	$\alpha_{\text{Cu(II)/Cu(I)}}$	Cu(II)/Cu(I) minerals
ODC20	1.00369	Ol/Fahl
Cu8	1.00182	Mal/Fahl
NNB91	1.00160	Mal/Fahl
Wein8438	1.00245	Chry/Ccp
Metz57	1.00197	Mal/Ccp
M2-2	1.00443	Mal/Ccp
NNB43	0.99844	Mal/Cup
Cu14	1.00051	Mal/Cup
Cu3	1.00036	Mal/Cup
ZBH37	0.99933	Mal/Cup

Note: The fractionation factor  $\alpha$  is defined in the text; mineral abbreviations: Ol, olivenite; Fahl, fahlore; Mal, malachite; Chry, chrysocolla; Ccp, chalcopyrite; Cup, cuprite.

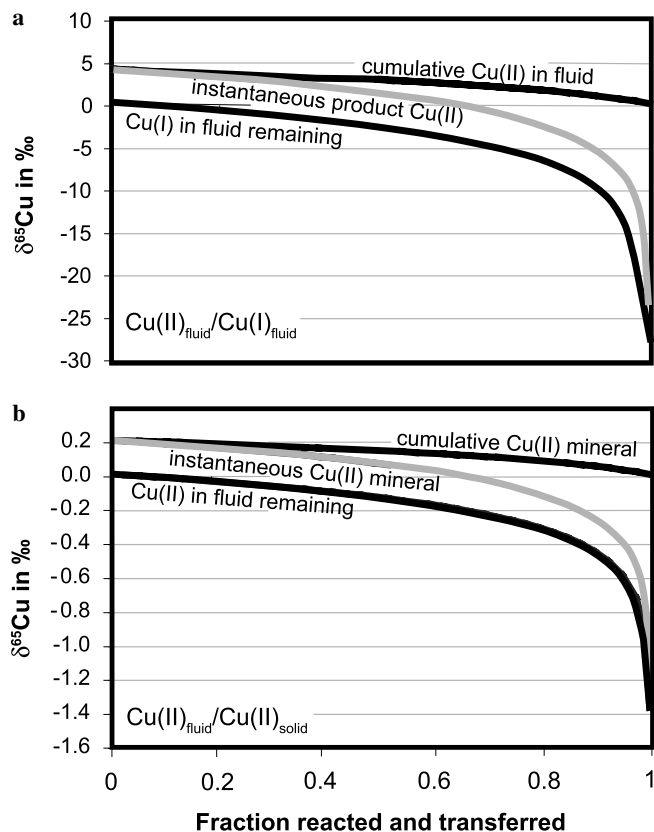


Fig. 6. The results of Rayleigh-type mass balance calculations using an initial fluid with a  $\delta^{65}\text{Cu}$  of zero. (a) A Cu(I)-bearing fluid is oxidized and Cu(II) is precipitated quantitatively e.g. as malachite; Cu(I)/Cu(II) fractionation in the fluid is governed by a fractionation factor of 1.004 as experimentally determined by Zhu et al. (2002). (b) A Cu(II)-bearing fluid precipitates a Cu(II) mineral; fractionation here is governed by the fluid–solid fractionation factor of 1.0002 as determined by Marechal and Sheppard (2002).  $F$  is the fraction of original species consumed.

closed system using the fractionation factors discussed above. It is obvious, that precipitation of a Cu(II) mineral from a Cu(II) solution normally does not produce the copper isotope values of secondary copper minerals that we measured. Fractionation within a Cu(I)- and Cu(II)-bearing fluid, however, would produce exactly the range of observed copper isotope values for secondary copper minerals for small to moderate  $F$  factors.

The large spread in isotopic values even within a single deposit raises the question about the attainment of equilibrium during the redox process. It is obvious both from the textures and from the isotope data that complete equilibrium was not attained even on a sample scale. However, as the calculated fractionation factors agree very closely with the experimental ones, the variation of  $\delta^{65}\text{Cu}$  and corresponding  $\alpha$  values may either indicate equilibrium processes on a much smaller scale ( $\mu\text{m}$  to  $\text{nm}$ ), or it may reflect the different importance of within–fluid (i. e. Cu(II)/Cu(I) ionic species) and fluid–solid equilibrium. The first of these possibilities would mean that the oxidative dissolution of primary Cu-sulfide involves the selective dissolution of heavy Cu isotopes from a leached layer, producing a Cu(II)

fluid enriched in  $^{65}\text{Cu}$  and leaving the residual Cu(I)-mineral enriched in the light isotope. While this mechanism was also suggested by Brantley et al. (2004) for Fe isotopes, Rouxel et al. (2005) prefer dissolution–reprecipitation instead of solid-state diffusion. More experimental work must be performed to really address this issue. The end member scenarios are defined by the experiments of Zhu et al. (2002, within–fluid) and Marechal and Sheppard (2002, fluid–solid) and their values correspond well to the extreme values found in our study. All values between these extreme values of 1.0002 (fluid–solid) and 1.004 (within–fluid) could be interpreted as a mixture of the two controlling processes. This would correspond to local equilibrium which is well-known from diffusion-controlled processes, e.g. during metamorphism (e.g. Fisher, 1975, 1977; Joesten, 1977; Markl et al., 1998). Alternatively, again mass balance considerations (see Fig. 6) could account for the observed spread in copper isotope compositions.

## 6. Summary and conclusions

$\delta^{65}\text{Cu}$  values of most fresh primary copper ores from the Schwarzwald, SW Germany, show only small variations around  $0 \pm 0.5\text{‰}$ , which points to a homogeneous fluid and negligible modifications during hydrothermal precipitation processes. Only two deposits in the northern Schwarzwald show lighter  $\delta^{65}\text{Cu}$  values of primary ores around  $-1.5 \pm 0.5\text{‰}$  and are therefore interpreted as having formed from recycled copper derived from older deposits.

Redox reactions lead to the formation of abundant secondary Cu(II) minerals with greatly variable  $\delta^{65}\text{Cu}$  values between  $-1$  and  $3\text{‰}$ , whereas the reaction of a primary to a secondary Cu(I) mineral such as cuprite does not appear to affect the  $\delta^{65}\text{Cu}$  value significantly. Also, reduction to native copper appears to retain the copper isotope composition of the precursor Cu(II) mineral. The oxidation process, by which isotopically heavier Cu(II) minerals form, leaves behind relics of the primary Cu(I) ores which are isotopically lighter. This points to selective preferential oxidation of the heavier copper isotope during low-temperature oxidation processes and to diffusion of  $^{65}\text{Cu}$  through the sulfide ore over distances of some millimeters or to small-scale dissolution–reprecipitation reactions. The large range in isotope compositions indicates that these redox processes do not reach sample-scale equilibrium (which is also shown by the mineral textures), but it can be interpreted as an interplay between two competing controls on the isotope fractionation process: within–fluid and fluid–solid fractionation. This indicates that the fractionation itself can probably be regarded as an equilibrium process on the nanometer-scale; otherwise, the distinction between Cu(I) and Cu(II) minerals would not be as sharp as observed. Similarly, a rate-controlled (i.e., kinetically controlled) process would not favour the mobilization and oxidation of the heavier isotope  $^{65}\text{Cu}$  which is shown by our data. Further investigations concerning the quantita-

tive effects of these two equilibrium processes should focus on the homogeneity within partly oxidized samples and on distribution patterns of  $\delta^{65}\text{Cu}$  values within single samples.

We conclude that copper isotopes may be a very helpful tool for unravelling details of redox processes in low-temperature systems (which may not only include ore deposits). Although the study of Graham et al. (2004) indicates that significant copper isotope fractionation occurs in magmatic–hydrothermal systems and that this can be used to a certain extent to fingerprint single intrusions, their results also showed considerable overlap in  $\delta^{65}\text{Cu}$  between the intrusions. Thus, copper isotopes cannot be easily used to track down a specific source of copper, be it in archaeological, geological or biological context, based on a single analysis of an artefact, a mineral or a biological sample.

### Acknowledgments

We thank Baatartsogt Baldorj and Anna Neumann for help during sample preparation. An earlier version of the manuscript was significantly improved by comments from Silke Severmann, Thomas Wagner, Derek Vance, Olivier Rouxel and three anonymous reviewers. We are very grateful for their careful reviews. The Associate Editor, Jeff Alt, is gratefully acknowledged for his friendly, careful and helpful handling of the manuscript.

Associate editor: Jeffrey C. Alt

### References

- Baatartsogt, B., Schwinn, G., Wagner, T., Taubald, H., Markl, G., in press. Contrasting paleofluid systems in the continental basement: a fluid inclusion and stable isotope study of hydrothermal vein mineralizations, Schwarzwald district, Germany. *Geofluids*.
- Bliedner, M., Martin, M., 1986. Erz- und Minerallagerstätten des Mittleren Schwarzwaldes. *Geol. Landesamt Baden-Württemberg, Freiburg*, 776.
- Brantley, S., Lermann, L., Guynn, R., Anbar, A., Icopini, G., Barling, J., 2004. Fe isotopic fractionation during mineral dissolution with and without bacteria. *Geochim. Cosmochim. Acta* **68**, 3189–3204.
- Brugger, J., McPhail, D., Black, J., Spiccia, L., 2001. Complexation of metal ions in brines: application of electronic spectroscopy in the study of the Cu(II)–LiCl–H<sub>2</sub>O system between 25 and 90 °C. *Geochim. Cosmochim. Acta* **65**, 2691–2708.
- Collings, M., Sherman, D., Ragnarsdóttir, K., 2000. Complexation of Cu<sup>2+</sup> in oxidized NaCl brines from 25 °C to 175 °C: results from in situ EXAFS spectroscopy. *Chem. Geol.* **167**, 65–73.
- Ehrlich, S., Butler, I., Halicz, L., Rickard, D., Oldroyd, A., Matthews, A., 2005. Experimental study of the copper isotope fractionation between aqueous Cu(II) and covellite, CuS. *Chem. Geol.* **209**, 259–270.
- Fisher, G.W., 1975. The thermodynamics of diffusion controlled metamorphic processes. In: Cooper, A.R., Heuer, A.H. (Eds.), *Mass Transport Phenomena in Ceramics*. Plenum Press, New York, pp. 111–122.
- Fisher, G.W., 1977. Non-equilibrium thermodynamics in metamorphism. In: Fraser, D.G. (Ed.), *Thermodynamics in Geology*. Reidel Publication Company, Boston, pp. 381–403.
- Gale, N.H., Woodhead, A., Stos-Gale, Z.A., Walder, A., Bowen, I., 1999. Natural variations detected in the isotopic composition of copper: possible applications to archaeology and geochemistry. *Intern. J. Mass Spectrom.* **184**, 1–9.
- Graham, S., Pearson, N., Jackson, S., Griffin, W., O'Reilly, S., 2004. Tracing Cu and Fe from source to porphyry: in situ determination of Cu and Fe isotope ratios in sulfides from the Grasberg Cu–Au deposit. *Chem. Geol.* **207**, 147–169.
- Hoefs, J., Emmermann, R., 1983. The oxygen isotope composition of Hercynian granites and pre-Hercynian gneisses from the Schwarzwald, SW Germany. *Contrib. Mineral. Petrol.* **83**, 320–329.
- Hofmann, B., Eikenberg, J., 1991. The Krunkelbach uranium deposit, Schwarzwald, Germany. Correlation of radiometric ages. *Econ. Geol.* **86**, 1031–1049.
- Jiang, S., Woodhead, J., Jimin, Y., Jlayong, P., Qiling, L., Nanping, W., 2002. A reconnaissance of Cu isotopic compositions of hydrothermal vein-type copper deposit, Jinman, Yunnan, China. *Chin. Sci. Bull.* **47**, 247–250.
- Joesten, R., 1977. Evolution of mineral assemblage zoning in diffusion metasomatism. *Geochim. Cosmochim. Acta* **41**, 649–670.
- Johnson, C., Beard, B., Albarede, F., 2004. Overview and general concepts. In: *Geochemistry of non-traditional stable isotopes. Review in Mineralogy and Geochemistry*, vol. 55, pp. 1–24.
- Kalt, A., Altherr, R., Hanel, M., 2000. The Variscan basement of the Schwarzwald. *Eur. J. Miner.* **12**, 1–44, Beih. 1.
- Larson, P., Maher, K., Ramos, F., Chang, Z., Gaspar, M., Meinert, L., 2003. Copper isotope ratios in magmatic and hydrothermal ore-forming environments. *Chem. Geol.* **201**, 337–350.
- Lippolt, H., Kirsch, H., 1994. Isotopic investigation of post-Variscan plagioclase sericitization in the Schwarzwald Gneiss massif. *Chem. Erde* **54**, 123–142.
- Liu, W., McPhail, D., Brugger, J., 2001. An experimental study of copper(I)-chloride and copper(I)-acetate complexing in hydrothermal solutions between 50 °C and 250 °C and vapor-saturated pressure. *Geochim. Cosmochim. Acta* **65**, 2937–2948.
- Luck, J.M., Ben Othman, D., Barrat, J., Albarede, F., 2003. Coupled 63Cu and 16O excesses in chondrites. *Geochim. Cosmochim. Acta* **67**, 143–151.
- Lüders, V., 1994. Geochemische Untersuchungen an gangartmineralen aus dem Bergbaurevier Freiamt-Sexau und dem Badenweiler-Quarzf. *Abh. Geol. Landesamt Baden-Württemberg* **14**, 173–190.
- Manhès, C., Minster, J.F., Allègre, C.J., 1978. Comparative uranium, thorium, lead, and strontium of St Severin amphotericite: consequences for early solar system chronology. *Earth Planet. Sci. Lett.* **39**, 14–24.
- Marechal, C., Albarede, F., 2002. Ion-exchange fractionation of copper and zinc isotopes. *Geochim. Cosmochim. Acta* **66**, 1499–1509.
- Marechal, C., Sheppard, S., 2002. Isotopic fractionation of Cu and Zn between chloride and nitrate solutions and malachite or smithsonite at 30 and 50 °C. Proceedings of the Goldschmidt-Conference, *Geochim. Cosmochim. Acta* **66**, 15A, A484.
- Marechal, C.N., Telouk, P., Albarede, F., 1999. Precise analysis of copper and zinc isotopic compositions by plasma-source mass spectrometry. *Chem. Geol.* **156**, 251–273.
- Markl, G., Foster, T., Bucher, K., 1998. Diffusion-controlled olivine corona textures in granitic rocks from Lofoten, Norway: calculation of Onsager diffusion coefficients, thermodynamic modelling and petrologic implications. *J. Metam. Geol.* **16**, 607–623.
- Markl, G., von Blanckenburg, F., Wagner, T., 2006. Iron isotope fractionation during hydrothermal ore deposition and alteration. *Geochim. Cosmochim. Acta* **70**, 3011–3030.
- Meshik, A., Lippolt, H., Dymkov, Y., 2000. Xenon geochronology of Schwarzwald pitchblendes. *Min. Deposita* **35**, 190–205.
- Metz, R., Richter, M., Schürenberg, H., 1957. Die Blei-Zink-Erzgänge des Schwarzwaldes. *Beih. Geol. Jb.* **29**, 277 p.
- Meyer, M., Brockamp, O., Clauer, N., Renk, A., Zuther, M., 2000. Further evidence for a Jurassic mineralizing event in central Europe: K–Ar dating of hydrothermal alteration and fluid inclusion systematics in wall rocks of the Käfersteige fluorite vein deposit in the northern Black Forest, Germany. *Miner. Deposita* **35**, 754–761.
- Mountain, B., Seward, T., 2003. Hydrosulphide/sulphide complexes of copper(I): Experimental confirmation of the stoichiometry and stability of Cu(HS)<sub>2</sub><sup>-</sup> to elevated temperatures. *Geochim. Cosmochim. Acta* **67**, 3005–3014.

- O'Nions, K., Zhu, X., 2002. Natural and experimental mass fractionation of transition metal isotopes. Proceedings of the Goldschmidt-Conference, *Geochim. Cosmochim. Acta* **66**, 15A, A563.
- Riuz, J., Mathur, R., Young, S., Brantley, S., 2002. Controls of copper isotope fractionation. Proceedings of the Goldschmidt-Conference, *Geochim. Cosmochim. Acta* **66**, 15A, A484.
- Rouxel, O., Fouquet, Y., Ludden, J., 2004. Copper isotope systematics of the lucky strike, rainbow, and logatchev sea-floor hydrothermal fields on the mid-Atlantic ridge. *Econ. Geol.* **90**, 585–600.
- Schwinn, G., Markl, G., 2005. REE systematics in hydrothermal fluorite. *Chem. Geol.* **216**, 225–248.
- Schwinn, G., Wagner, T., Baatartsoyt, B., Markl, G., 2006. Quantification of mixing processes in ore-forming hydrothermal systems by combination of stable isotope and fluid inclusion analyses. *Geochim. Cosmochim. Acta* **70**, 965–982.
- Segev, A., Halicz, L., Lang, B., Steinitz, G., 1991. K–Ar dating of manganese minerals from the Eisenbach region, Black Forest, southwest Germany. *Schweiz. Min. petrogr. Mitt.* **71**, 101–114.
- Seyfried, W., Ding, K., 1993. The effect of redox on the relative solubilities of copper and iron in Cl-bearing aqueous fluids at elevated temperatures and pressures: An experimental study with application to subseafloor hydrothermal systems. *Geochim. Cosmochim. Acta* **57**, 1905–1917.
- Shields, W.R., Goldich, S.S., Garner, E.L., Murphy, T.J., 1965. Natural variations in the abundance ratio and the atomic weight of copper. *J. Geophys. Res.* **70**, 479–491.
- Simon, K., Hoefs, J., 1987. Effects of meteoric water interaction on Hercynian granites from the Südschwarzwald, southwest Germany. *Chem. Geol.* **61**, 253–261.
- Wagner, T., Cook, N., 2000. Late-Variscan antimony mineralization in the Rheinisches Schiefergebirge, NW Germany: evidence for stibnite precipitation by drastic cooling of high-temperature fluid systems. *Miner. Deposita* **35**, 206–222.
- Walker, E.C., Cuttitta, F., Senftle, F.E., 1958. Some natural variations in the relative abundance of copper isotopes. *Geochim. Cosmochim. Acta* **15**, 183–194.
- Werner, W., Franzke, H.J., 1994. Tektonik und Mineralisation der Hydrothermalgänge am Schwarzwaldrand im Bergbaurevier Freiamt-Sexau. *Abh. Geol. Landesamt Baden-Württemberg* **14**, 27–98.
- Werner, W., Franzke, H. J., Wirsing, G., Jochum, J., Lüders, V., Wittenbrink, J., 2000. Die Erzlagerstätte Schauinsland bei Freiburg im Breisgau. *Aedificatio-Verlag*, Freiburg, 110 S.
- Wernicke, R., Lippolt, H., 1994. Dating of vein specularite using internal (U+Th)/4He isochrons. *Geophys. Res. Lett.* **21**, 345–347.
- Wernicke, R., Lippolt, H., 1997. (U+Th)-He evidence of Jurassic continuous hydrothermal activity in the Schwarzwald basement, Germany. *Chem. Geol.* **138**, 273–285.
- Xiao, Z., Gammons, C., Williams-Jones, A., 1998. Experimental study of Copper(I) chloride complexing in hydrothermal solutions at 40 to 300 °C and saturated water vapor pressure. *Geochim. Cosmochim. Acta* **62**, 2949–2964.
- Zhu, X., Guo, Y., Williams, R., O'Nions, K., Matthews, A., Belshaw, N., Canters, G., de Waal, E., Weser, U., Burgess, B., Salvato, B., 2002. Mass fractionation processes of transition metal isotopes. *Earth Planet. Sci. Lett.* **200**, 47–62.
- Zhu, X., O'Nions, K., Guo, Y., Belshaw, N., Rickard, D., 2000. Determination of natural Cu-isotope variation by plasma-source mass spectrometry: implications for use as geochemical tracers. *Chem. Geol.* **163**, 139–149.
- Zuther, M., Brockamp, O., 1988. The fossil geothermal system of the Baden-Baden trough (Northern Black Forest, Germany). *Chem. Geol.* **71**, 337–353.